Electronic Supporting Information

Hierarchiral Tandem Assembly of Planar [3×3] Building Units into {3×[3×3]} Oligomers: Mixed-Valency, Electrical Conductivity and Magnetism

Fei Yu,[†] Mohamedally Kurmoo,[§] Gui-Lin Zhuang,[‡] and Jing-Lin Zuo[*,†]

[†] State Key Laboratory of Coordination Chemistry, School of Chemistry and Chemical Engineering, Collaborative Innovation Center of Advanced Microstructures, Nanjing University, Nanjing, 210023, P.R. China.

[§] Institut de Chimie de Strasbourg, Université de Strasbourg, CNRS-UMR 7177, 4 rue Blaise Pascal, 67008 Strasbourg, France.

[‡] College of Chemical Engineering, Zhejiang University of Technology, Hangzhou, 310032, P.R. China.

*Email: zuijl@nju.edu.cn

Table S1. Selected bond lengths (Å) and angles (°) for **Cu₉** and **Cu₂₇**.

Cu₉			
Cu1-N1	2.025(5)	Cu1-N2	1.924(4)
Cu1-N15	1.937(4)	Cu1-N16	1.969(5)
Cu2-N3	1.967(5)	Cu2-N3^i	1.967(5)
Cu2-N4	1.952(5)	Cu2-N4^i	1.952(5)
Cu3-N5	1.911(5)	Cu3-N6	2.020(5)
Cu3-N9	1.968(5)	Cu3-N10	1.931(5)
Cu4-N7^i	2.066(6)	Cu4-N7	2.066(6)
Cu4-N8^i	1.917(6)	Cu4-N8	1.917(6)
Cu5-N11	2.011(5)	Cu5-N12	2.036(6)
Cu5-N13^i	2.047(5)	Cu5-N14^i	2.006(5)
Cu6-N17^i	1.919(5)	Cu6-N17	1.919(5)
Cu6-N18	2.053(7)	Cu6-N18^i	2.053(7)
N2-Cu1-N1	81.1(2)	N2-Cu1-N15	161.4(2)
N2-Cu1-N16	103.1(2)	N15-Cu1-N1	104.6(2)
N15-Cu1-N16	80.8(2)	N16-Cu1-N1	150.0(2)
N3-Cu2-N3^i	149.0(3)	N4-Cu2-N3	81.6(2)
N4^i-Cu2-N3^i	81.6(2)	N4^i-Cu2-N3	106.6(2)
N4-Cu2-N3^i	106.6(2)	N4-Cu2-N4^i	149.9(3)
N5-Cu3-N6	80.9(2)	N5-Cu3-N9	103.6(2)
N5-Cu3-N10	161.4(2)	N9-Cu3-N6	150.3(2)
N10-Cu3-N6	104.2(2)	N10-Cu3-N9	80.9(2)
N7^i-Cu4-N7	140.6(3)	N8-Cu4-N7	80.9(2)
N8^i-Cu4-N7^i	80.9(2)	N8^i-Cu4-N7	105.2(2)
N8-Cu4-N7^i	105.2(2)	N8^i-Cu4-N8	162.2(3)
N11-Cu5-N12	80.8(2)	N11-Cu5-N13^i	141.2(2)
N12-Cu5-N13^i	114.7(2)	N14^i-Cu5-N11	106.3(2)
N14^i-Cu5-N12	146.0(2)	N14^i-Cu5-N13^i	80.9(2)
N17^i-Cu6-N17	160.5(3)	N17-Cu6-N18	81.0(2)
N17^i-Cu6-N18	105.3(2)	N17-Cu6-N18^i	105.3(2)
N17^i-Cu6-N18^i	81.0(2)	N18^i-Cu6-N18	143.2(3)

	Cu27		
Cu1-N1	2.007(5)	Cu1-N2	2.037(5)
Cu1-N19	1.995(5)	Cu1-N20	2.061(5)
Cu1-O2	1.970(9)	Cu1-O2'	2.031(6)
Cu2-N3	1.994(5)	Cu2-N4	2.221(5)
Cu2-N25	2.031(5)	Cu2-N26	1.981(5)
Cu2-N109	1.969(6)	Cu2-C289	1.969(6)
Cu3-N5	1.963(5)	Cu3-N6	2.310(5)
Cu3-N31	2.069(5)	Cu3-N32	1.940(5)
Cu3-N111	1.950(7)	Cu3-C291	1.950(7)
Cu4-N7	2.022(5)	Cu4-N8	1.988(5)
Cu4-N21	1.972(5)	Cu4-N22	2.223(5)
Cu4-N118	1.992(6)	Cu4-C298	1.992(6)
Cu5-N9	1.956(5)	Cu5-N10	1.960(5)
Cu5-N27	1.954(5)	Cu5-N28	1.958(5)
Cu6-N11	1.924(5)	Cu6-N12	2.072(5)
Cu6-N33	1.941(5)	Cu6-N34	1.969(5)
Cu7-N13	2.058(6)	Cu7-N14	1.944(5)
Cu7-N23	1.956(5)	Cu7-N24	2.285(6)
Cu7-N120	1.971(7)	Cu7-C300	1.971(7)
Cu8-N15	1.937(5)	Cu8-N16	1.980(5)
Cu8-N29	1.905(5)	Cu8-N30	2.071(5)
Cu9-N17	1.943(5)	Cu9-N18	2.121(6)
Cu9-N35	1.927(5)	Cu9-N36	2.136(5)
Cu10-N37	1.970(5)	Cu10-N38	2.044(5)
Cu10-N55	2.000(5)	Cu10-N56	2.060(5)
Cu10-O1	2.034(10)	Cu10-O1'	2.005(6)
Cu11-N39	1.961(5)	Cu11-N40	2.227(5)
Cu11-N61	2.014(5)	Cu11-N62	1.992(5)
Cu11-N113	1.984(6)	Cu11-C293	1.984(6)
Cu12-N41	1.946(6)	Cu12-N42	2.254(7)
Cu12-N67	2.048(5)	Cu12-N68	1.992(5)
Cu12-N115	1.966(7)	Cu12-C295	1.966(7)

Cu13-N43	2.023(5)	Cu13-N44	1.999(5)
Cu13-N57	1.972(5)	Cu13-N58	2.257(6)
Cu13-N110	1.982(6)	Cu13-C290	1.982(6)
Cu14-N45	1.942(5)	Cu14-N46	1.960(5)
Cu14-N63	1.969(5)	Cu14-N64	1.969(5)
Cu15-N47	1.895(5)	Cu15-N48	2.070(5)
Cu15-N69	1.927(6)	Cu15-N70	1.984(5)
Cu16-N49	2.066(7)	Cu16-N50	1.924(6)
Cu16-N59	1.958(6)	Cu16-N60	2.219(7)
Cu16-N112	1.946(6)	Cu16-C292	1.946(6)
Cu17-N51	1.938(6)	Cu17-N52	1.978(6)
Cu17-N65	1.925(5)	Cu17-N66	2.070(6)
Cu18-N53	1.900(6)	Cu18-N54	2.113(6)
Cu18-N71	1.921(5)	Cu18-N72	2.124(7)
Cu19-N73	2.004(5)	Cu19-N74	2.035(5)
Cu19-N91	2.004(5)	Cu19-N92	2.059(5)
Cu19-O3	2.042(10)	Cu19-O3'	2.061(6)
Cu20-N75	1.970(5)	Cu20-N76	2.230(5)
Cu20-N97	2.027(5)	Cu20-N98	1.977(5)
Cu20-N117	2.003(6)	Cu20-C297	2.003(6)
Cu21-N77	1.955(5)	Cu21-N78	2.296(5)
Cu21-N103	2.048(6)	Cu21-N104	1.937(5)
Cu21-N119	1.956(6)	Cu21-C299	1.956(6)
Cu22-N79	2.022(5)	Cu22-N80	1.972(5)
Cu22-N93	1.975(5)	Cu22-N94	2.251(5)
Cu22-N114	1.988(6)	Cu22-C294	1.988(6)
Cu23-N81	1.962(5)	Cu23-N82	1.941(5)
Cu23-N99	1.964(5)	Cu23-N100	1.945(5)
Cu24-N83	1.910(5)	Cu24-N84	2.074(5)
Cu24-N105	1.939(5)	Cu24-N106	1.975(5)
Cu25-N85	2.052(6)	Cu25-N86	1.937(5)
Cu25-N95	1.957(5)	Cu25-N96	2.226(5)
Cu25-N116	1.998(6)	Cu25-C296	1.998(6)

Cu26-N87	1.939(5)	Cu26-N88	1.971(5)
Cu26-N101	1.919(5)	Cu26-N102	2.071(5)
Cu27-N89	1.926(5)	Cu27-N90	2.153(5)
Cu27-N107	1.918(5)	Cu27-N108	2.159(5)
N109(C289)-C290(N110)	1.206(8)	N111(C291)-C292(N112)	1.194(8)
N113(C293)-C294(N114)	1.168(8)	N115(C295)-C296(N116)	1.147(8)
N117(C297)-C298(N118)	1.154(7)	N119(C299)-C300(N120)	1.160(8)

Symmetry code for **Cu$_9$**: (i) $-x+1, y, -z+1/2$; (ii) $-x+1, -y+1, -z+1$; (iii) $-x+1, y, -z+1/2$.

Table S2. Hydrogen-bond geometry (Å, º) for **Cu$_9$**. (D, donor atom; A, acceptor atom).

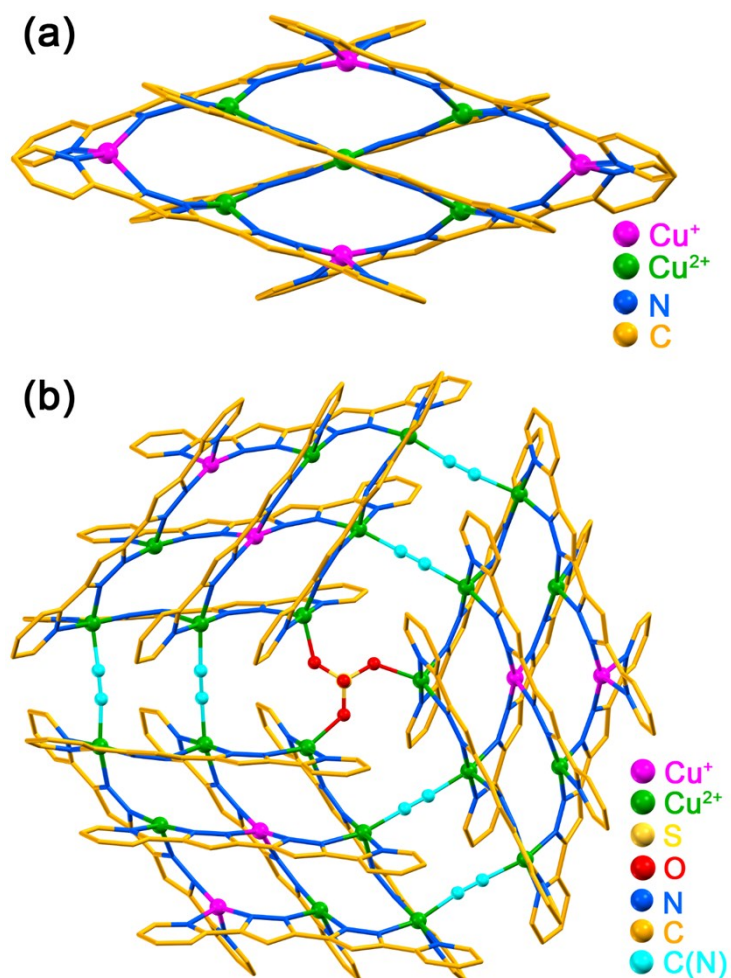| D-H$\cdots A$	$D\cdots A$	D-H$\cdots A$
C45-H45$\cdots$O3^{ii}	3.521(18)	165
C31-H31$\cdots$O1^{iii}	3.32(3)	135
C42-H42$\cdots$O3^{ii}	3.428(17)	158
C49-H49$A\cdots$O4^{iv}	2.66(4)	139

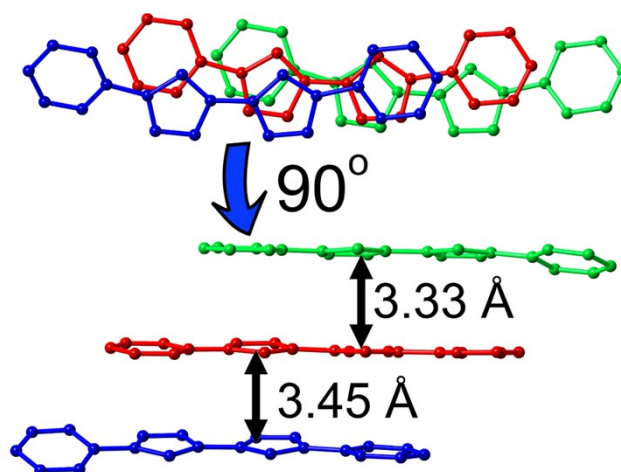Symmetry codes: (ii) $-x+1, -y+1, -z+1$; (iii) $-x+3/2, -y+3/2, -z+1$; (iv) $-x+3/2, -y+5/2, -z+1$.
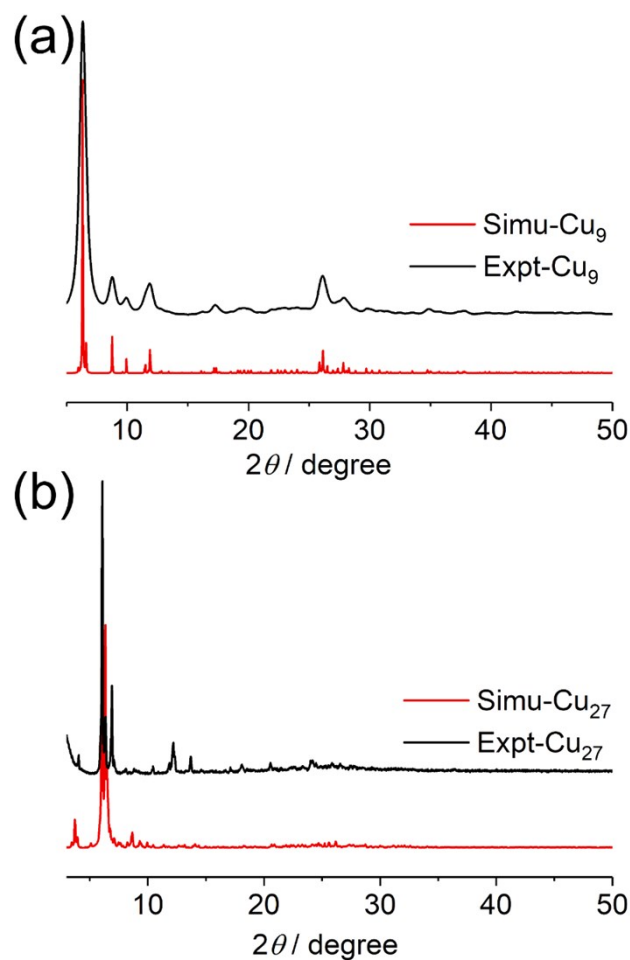
Fig. S1. Experimental (Expt.) and simulated (Simu.) PXRD patterns of (a) **Cu₉** and (b) **Cu₂₇**.
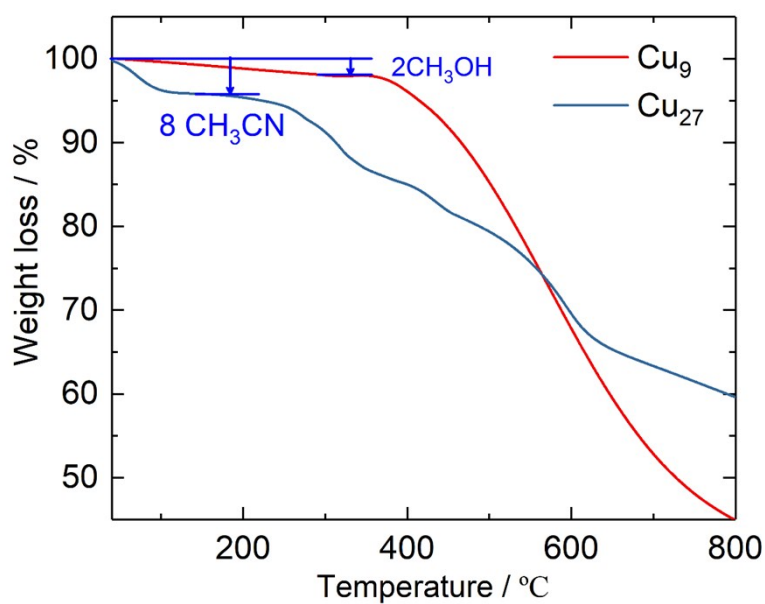
**Fig. S2**. Thermogravimetric analyses of **Cu₉** and **Cu₂₇** under N_2. The heating rate was 5 °C min^{-1} from 40 to 800 °C.

Fig. S3. Views of the crystal structure of (a) **Cu$_9$** and (b) **Cu$_{27}$**. SO$_4^{2-}$ anion, and CH$_3$OH for **Cu$_9$**, CH$_3$CN for **Cu$_{27}$** molecules are omitted for clarity.

Fig. S4. Views of the intramolecular overlap of the ligands on one face of a **Cu$_9$** molecule showing the average interplanar distances, shorter than the van der Waal sum of the atomic radii.
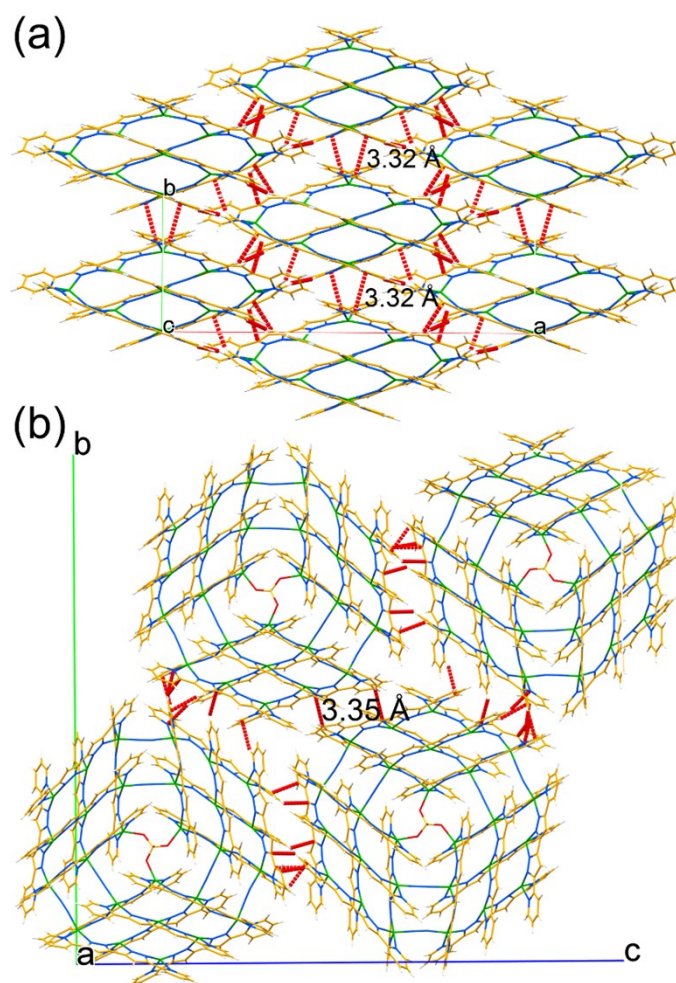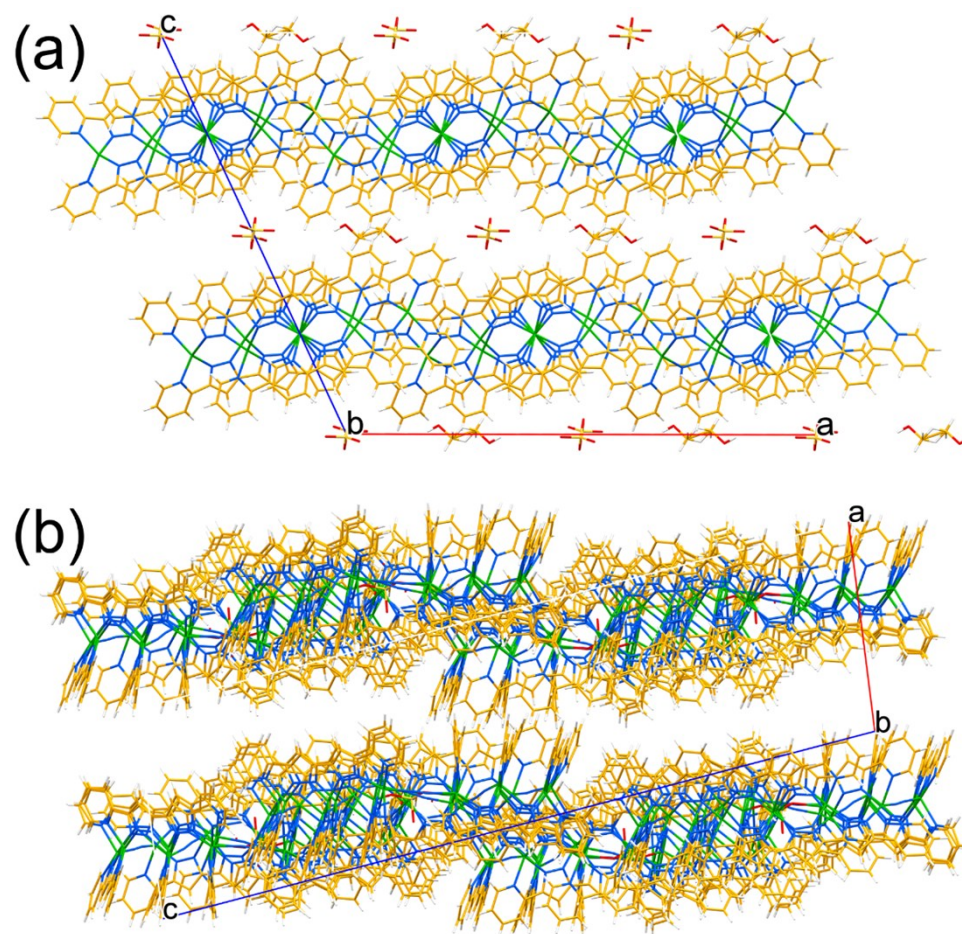
Fig. S5. Views of the crystal packing along the (a) *ab*-plane of **Cu₉** and (b) *bc*-plane of **Cu₂₇** showing the short intermolecular interactions in solid red lines; SO_4^{2-} anion, and CH_3OH for **Cu₉**, CH_3CN for **Cu₂₇** molecules are omitted for clarity.

**Table S3**. Intermolecular interactions (Å) for **Cu₉** and **Cu₂₇**.

	C-H···π	Distance (Å)	C-H···π	Distance (Å)
Cu₉	C33-H33···π	2.727	C36-H36···π	2.878
	C16-H16···π	2.879	π···π	3.32
Cu₂₇	C14-H14···π	2.889	C15-H15···π	2.702
	C16-H16···π	2.798	C31-H31···π	2.849
	C48-H48···π	2.896	C64-H64···π	2.834
	C79-H79···π	2.803	C94-H94···π	2.847
	C95-H95···π	2.720	C142-H142···π	2.781
	C143-H143···π	2.796	C223-H223···π	2.738

	C224-H224⋯π	2.885	π⋯π	3.35

Fig. S6. Views of the crystal packing for **Cu$_9$** (a) and **Cu$_{27}$** (b) in the *ac*-plane; SO$_4^{2-}$ anion, and CH$_3$CN for **Cu$_{27}$** molecules are omitted for clarity.
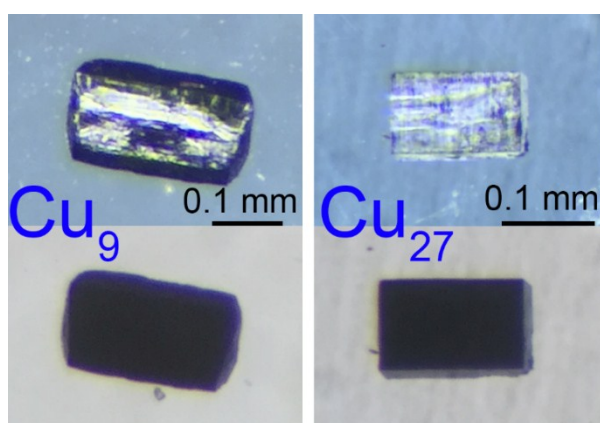
Fig. S7. Views of the single crystals of **Cu$_9$** (left) and **Cu$_{27}$** (right) under a microscope with reflecting (top) and transmitting (bottom) light. The single crystals of **Cu$_9$** and **Cu$_{27}$** appear metallic under reflecting light.
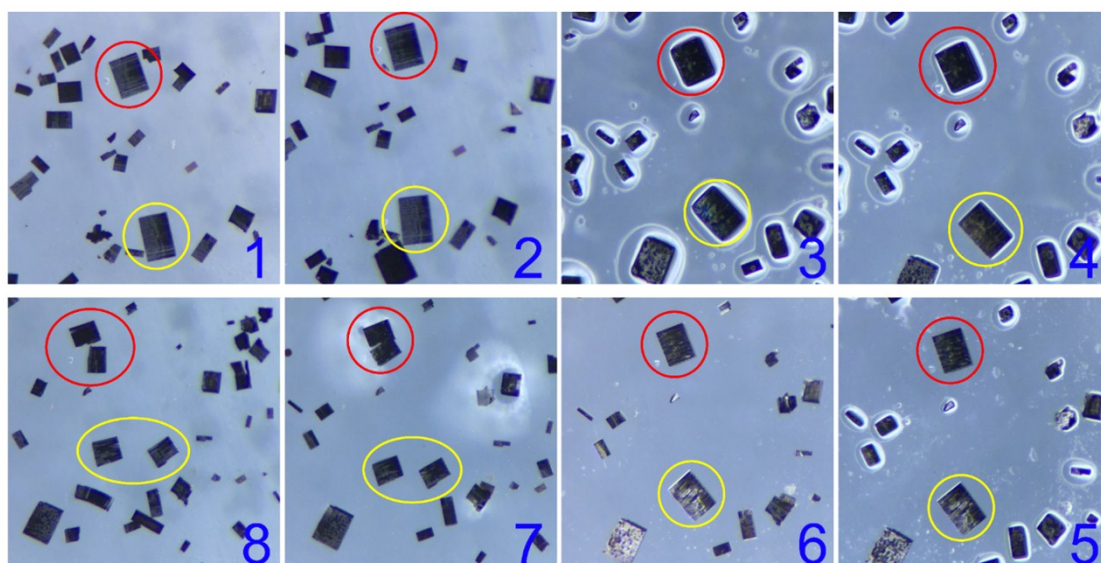
Figure S8. Views of the crystals of **Cu₂₇** under a microscope by using reflecting light. Frames 1 and 2 were in CH₃OH, 3, 4 and 5 were taken during the solvent drying, 6 was after completely dried, and for 7 and 8 a drop of CH₃OH was added. Red and yellow circles follow two individual crystals during the process. Note the lines on the crystals along which the cleavage takes place.
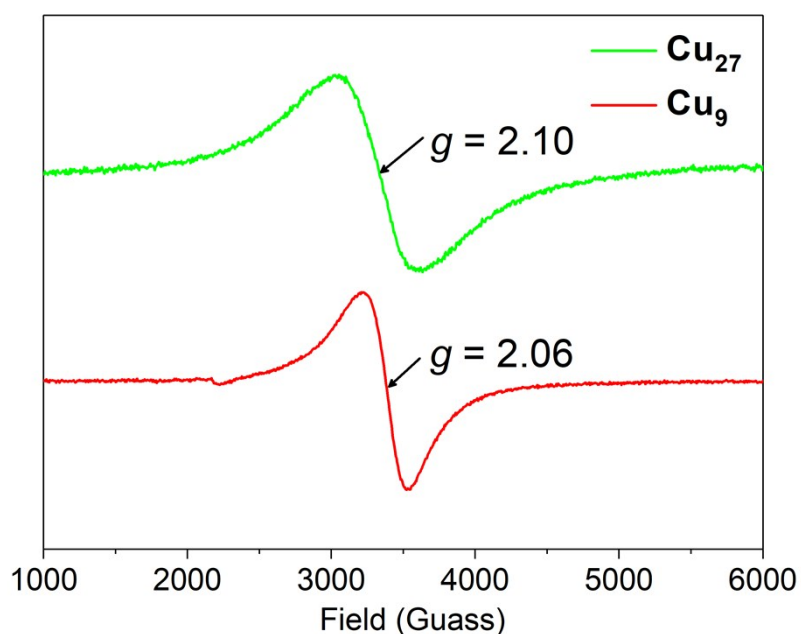

Fig. S9. X-band EPR spectra of randomly oriented polycrystalline samples of **Cu₉** and **Cu₂₇** at 298 K, at a microwave frequency of 9.545 GHz and power of 0.189 mW.

Table S4. Spin population of **Cu₉** and **Cu₂₇**.

Cu9	Cu1	Cu2	Cu3	Cu4	Cu5	Cu6	Cu1'	Cu3'	Cu5'
Alpha population	9.40328	9.39976	9.26015	9.36714	9.33358	9.36969	9.40335	9.40006	9.33357
Beta population	8.91883	8.87610	8.82197	9.13362	9.31549	9.13868	8.91898	8.87653	9.31546
Spin population	0.48444	0.52366	0.43818	0.23352	0.01809	0.23101	0.48437	0.52353	0.01810
Atomic charge	0.67789	0.72414	0.91787	0.49924	0.35093	0.49164	0.67767	0.72341	0.35097
Evaluated oxidation state	+2	+2	+2	+1	+1	+1	+2	+2	+1

Cu27	Cu1	Cu2	Cu3	Cu4	Cu5	Cu6	Cu7	Cu8	Cu9
Alpha population	9.37921	9.45696	9.48018	9.42192	9.13984	9.35504	9.42855	9.36269	9.27814
Beta population	8.74797	8.88571	8.93338	8.82927	8.74633	8.86087	8.86652	8.87054	9.25743
Spin population	0.63123	0.57125	0.54680	0.59264	0.39351	0.49416	0.56203	0.49214	0.02071
Atomic charge	0.87282	0.65732	0.58644	0.74881	1.11382	0.78409	0.70493	0.76677	0.46442
Evaluated oxidation state	+2	+2	+2	+2	+1	+2	+2	+2	+1
Cu27	Cu10	Cu11	Cu12	Cu13	Cu14	Cu15	Cu16	Cu17	Cu18
Alpha population	9.38561	9.46617	9.49332	9.41555	9.12893	9.35889	9.37921	9.35761	9.28810
Beta population	8.75529	8.89399	8.94874	8.82281	8.74096	8.84700	8.74797	8.87610	9.26189
Spin population	0.63033	0.57218	0.54457	0.59273	0.38797	0.51189	0.63123	0.48151	0.02620
Atomic charge	0.85910	0.63984	0.55794	0.76164	1.13011	0.79411	0.87282	0.76629	0.45001
Evaluated oxidation state	+2	+2	+2	+2	+1	+2	+2	+2	+1
Cu27	Cu19	Cu20	Cu21	Cu22	Cu23	Cu24	Cu25	Cu26	Cu27
Alpha population	9.36735	9.48348	9.47967	9.41059	9.13411	9.35022	9.43811	9.33724	9.30031
Beta	8.74018	8.91101	8.93246	8.80813	8.73458	8.84895	8.88548	8.87469	9.26192

population									
Spin population	0.62717	0.57247	0.54721	0.60246	0.39953	0.50127	0.55263	0.46256	0.03839
Atomic charge	0.89247	0.60551	0.58787	0.78127	1.13130	0.80083	0.67641	0.78807	0.43777
Evaluated oxidation state	+2	+2	+2	+2	+1	+2	+2	+2	+1
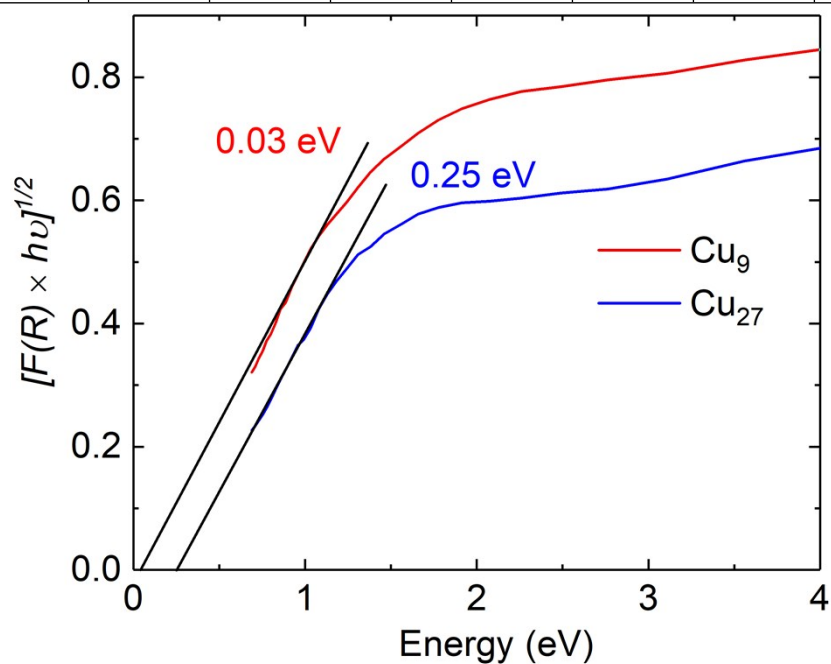
Fig. S10. Tauc plots of $[F(R)h\nu]^{1/2}$ *vs* $[h\nu]$ for the bandgap sizes of **Cu₉** (red) and **Cu₂₇** (blue) showing the crude extrapolation to estimate the bandgaps.